Nonequilibrium dynamics of a pure dry friction model subjected to colored noise

Paul M. Geffert and Wolfram Just
School of Mathematical Sciences, Queen Mary University of London, London E1 4NS, United Kingdom
(Received 8 November 2016; published 8 June 2017)

We investigate the impact of noise on a two-dimensional simple paradigmatic piecewise-smooth dynamical system. For that purpose, we consider the motion of a particle subjected to dry friction and colored noise. The finite correlation time of the noise provides an additional dimension in phase space, causes a nontrivial probability current, and establishes a proper nonequilibrium regime. Furthermore, the setup allows for the study of stick-slip phenomena, which show up as a singular component in the stationary probability density. Analytic insight can be provided by application of the unified colored noise approximation, developed by Jung and Hänggi [Phys. Rev. A **35**, 4464(R) (1987)]. The analysis of probability currents and of power spectral densities underpins the observed stick-slip transition, which is related with a critical value of the noise correlation time.

DOI: 10.1103/PhysRevE.95.062111

I. INTRODUCTION

Piecewise-smooth dynamical systems have attracted a lot of interest in the past decade. They are widely used to model switching or impact behavior in many different areas of science, e.g., biology, engineering, physics, or mathematics [1–5]. Systems with dry (or Coulomb) friction are prominent examples in the context of piecewise-smooth models [6]. The main feature of this type of friction is that an applied force has to overcome a certain threshold to move an object (sliding), otherwise the object rests (sticking) [7]. This behavior is usually modeled by a sign function, and it allows a simple macroscopic description for systems where solid-solid interactions are important, e.g., for stick-slip dynamics [8,9]. Adding noise to the dynamical equations of a piecewise-smooth system opens a whole new area of research, which is still in its infancy. The interplay of dry friction and random forces has been reported in [10–12]. Exact solutions are known for a few piecewise-smooth stochastic models, where, e.g., the propagator can be obtained for the case of pure dry friction [13,14] or in connection with Laplace transforms [15]. Other analytical results are available in the framework of path integrals and weak noise approximations [16–18] or first passage time problems [19]. Whereas the aforementioned studies are dealing with Gaussian white noise, models with Non-Gaussian noise and dry friction have been investigated as well [20–22]. The features of systems with dry friction subjected to random forces have also been observed in experimental setups [23–27]. From a more rigorous mathematical point of view, the impact of a stochastic perturbation on a piecewise-smooth dynamical system has been considered in [28,29].

A profound understanding of the impact of noise on piecewise-smooth dynamical systems is desirable from an intrinsic theoretical perspective, and it will contribute as well to relevant experimental issues. For instance, nonequilibrium properties of granular media are a topical subject; see, e.g., [30] for recent experimental results. The corresponding theoretical modeling uses granular material as a nonequilibrium heat bath, and the impact on devices subjected to dry friction is studied. Localization phenomena of the velocity and intermittent dynamics are consequences of the underlying stick-slip dynamics [31–33]. Realistic theoretical models are fairly complicated, thus only very limited analytic insight can be obtained.

The inclusion of a finite correlation time of the noise is a simple way to emulate nonequilibrium properties of a heat bath. If the correlation time of the noise is of the same order as the characteristic time scale of the system, a correlated noise (or colored noise) is required [34]. Analytical treatments of colored noise are hampered by the lack of detailed balance. In this context, the so-called unified colored noise approximation (UCNA) has been developed by Jung and Hänggi to obtain analytic expressions for the stationary probability density [35]. Colored noise has been studied in many different contexts, e.g., magnetic resonance systems [36] or neurodynamics [37].

The purpose of our contribution is twofold. We want to investigate the impact of noise on piecewise-smooth dynamical systems in a simple setup that allows for a partial analytic treatment. Furthermore, the nonequilibrium aspects, the occurrence of stationary probability currents, and transition phenomena will be a crucial part of our investigations. This paper is organized as follows: Section II introduces the pure dry friction model subjected to colored noise. The stationary behavior of the model is investigated in Sec. III. Analytic expressions for the velocity distribution will be derived together with an asymptotic expression for the two-dimensional stationary distribution. Analytic results are supported by numerical simulations for the density and for the stationary probability current. Dynamical properties such as the power spectral density and the distributions of sliding and sticking events are elaborated on in Sec. IV. We conclude our studies in Sec. V.

II. THE MODEL

We consider the simplest two-dimensional case of a piecewise-smooth stochastic system, which does not obey detailed balance. To motivate our considerations, let us recall the one-dimensional motion of a particle subjected to white noise. With a slight abuse of notation, the corresponding Langevin equation governing the velocity reads

$$\dot{v}(t) = -\sigma_0(v(t)) + \xi(t), \tag{1}$$

where $\xi(t)$ denotes a white Gaussian noise with correlation function $\langle \xi(t)\xi(s)\rangle = \delta(t-s)$, and $\sigma_0(v) = \mathrm{sgn}(v)$ contains

the deterministic part caused by Coulomb friction. We have adopted units such that the noise intensity and the dry friction coefficient have been normalized to 1. Equation (1) is not well defined at $v = 0$. One could cure such an inconsistency by considering the Coulomb friction as the limiting case of the regular drift $\sigma_\varepsilon(v) = \tanh(v/\varepsilon)$ for $\varepsilon \to 0$. Such niceties are not relevant for Eq. (1) as the white noise is not a function with well-defined finite values, and the stochastic model in a strict sense is not pointwise defined. The formally written down Fokker-Planck equation with suitable matching conditions ensuring continuity of the density and continuity of the probability current captures all aspects of the dynamics and has been studied intensely in the literature; see, e.g., [11]. The deterministic part without noise requires a more careful approach in terms of piecewise-smooth dynamical systems [1], particularly in the presence of a finite amplitude driving force where stick-slip transitions occur [cf. Eq. (3)].

An obvious extension of the model described above, leading toward a two-dimensional stochastic nonequilibrium system, consists in studying the effect of colored noise. To be precise, we intend to replace the Gaussian white noise by an exponentially correlated Ornstein-Uhlenbeck process $\eta(t)$, which is governed by the stochastic differential equation

$$\dot{\eta}(t) = -\frac{\eta(t)}{\tau} + \frac{\xi(t)}{\tau}. \tag{2}$$

The noise correlation time τ will be the only effective parameter in our model. Since the process $\eta(t)$ can be viewed as a continuous function, some care is needed when introducing the dynamics of the particle. For forces smaller than the dry friction coefficient, $|\eta| < 1$, and $v = 0$, the particle will stick while otherwise the sliding dynamics is still described by the aforementioned equation of motion.

Thus we end up with

$$\dot{v}(t) = \begin{cases} 0 & \text{if } v = 0 \text{ and } |\eta(t)| < 1, \\ -\sigma_0(v(t)) + \eta(t) & \text{otherwise.} \end{cases} \tag{3}$$

Alternatively, we could use the regularized drift

$$\dot{v}(t) = -\sigma_\varepsilon(v(t)) + \eta(t) \tag{4}$$

and consider results finally in the limit $\varepsilon \to 0$. We will adopt both views throughout our exposition while at the same time avoiding the considerable technical difficulties that would be related with a rigorous approach. Since we consider a noise with finite correlation time but a damping that does not involve a memory kernel, the system violates detailed balance and describes a nonequilibrium process [38]. On the contrary, the model in the white-noise limit, Eq. (1), has a vanishing stationary probability current and describes a process in equilibrium.

For the model defined by Eq. (3), the static friction equals the kinetic friction. In the real world the former exceeds the latter, and our assumption has to be considered as an idealization from an experimental perspective. Our particular choice does not include any hysteresis, but it has the advantage that the piecewise-smooth dynamical system can be captured as a singular limit of the smooth dynamics Eq. (4). Equation (3) provides the simplest consistent version of a piecewise-smooth dynamical system with a sliding region and an invisible tangent point [1]. Above all the model captures stick-slip phenomena, which will be a key ingredient of our analysis.

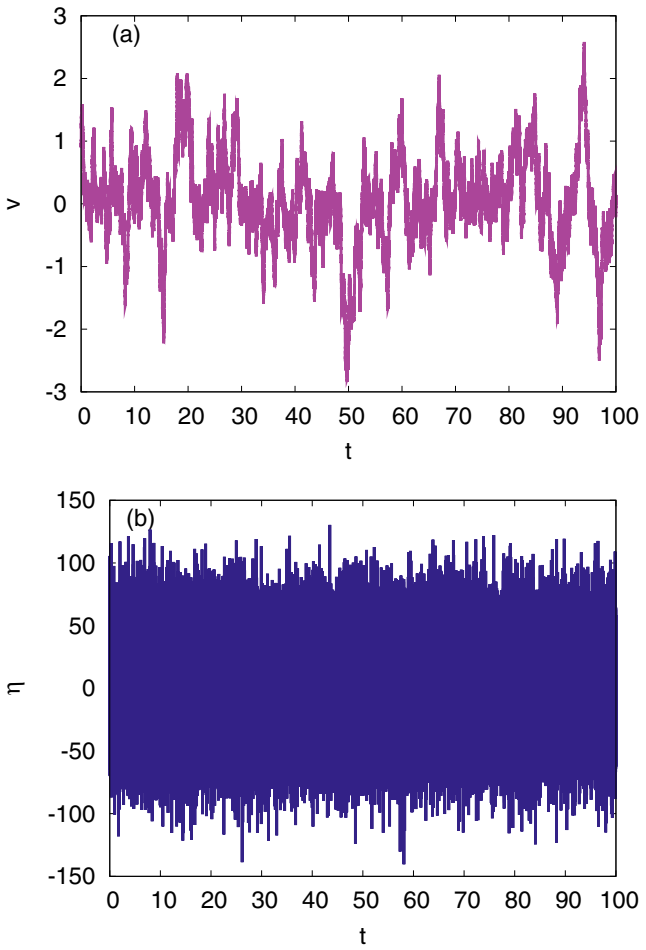

FIG. 1. Time traces of the velocity $v(t)$ (a) and the Ornstein-Uhlenbeck noise $\eta(t)$ (b) of the dry friction model [Eqs. (2) and (3)] for $\tau = 0.001$.

Before we enter a more detailed discussion, let us just illustrate the main phenomenon by time traces obtained from numerical simulations. Throughout all our numerical investigations, we apply an Euler-Maruyama scheme with step size $h = 10^{-3}$ for different values of τ. To take the discontinuity caused by dry friction into account [see Eq. (3)], we set $v = 0$ for $|v| < 10^{-3}$ and $|\eta| < 1$, as the particle sticks in this case at the origin. Time traces from the simulations are shown in Figs. 1–3. At a scale of order 1, the effect of dry friction becomes visible for correlation times larger than $\tau = 0.1$. The particle sticks for considerable amounts of time at $v = 0$, as the stochastic force $\eta(t)$ is not large enough to move the particle. It is this stick-slip phenomenon and the related intermittent motion that will be at the center of our studies, being the key signature of our piecewise-smooth stochastic model.

The observed dynamics from the simulations seems to be a key feature of dry friction subjected to noise and of general piecewise-smooth stochastic dynamics. Signatures of such intermittent dynamics have been found in the framework of the Boltzmann-Lorentz equation by investigating the so-called

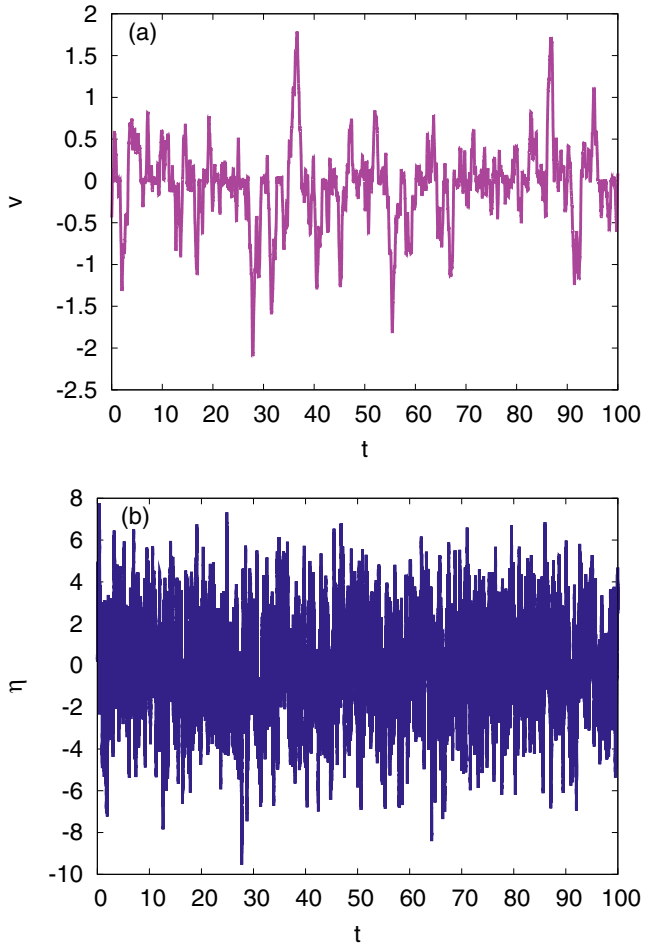

FIG. 2. Time traces of the velocity $v(t)$ (a) and the Ornstein-Uhlenbeck noise $\eta(t)$ (b) of the dry friction model [Eqs. (2) and (3)] for $\tau = 0.1$.

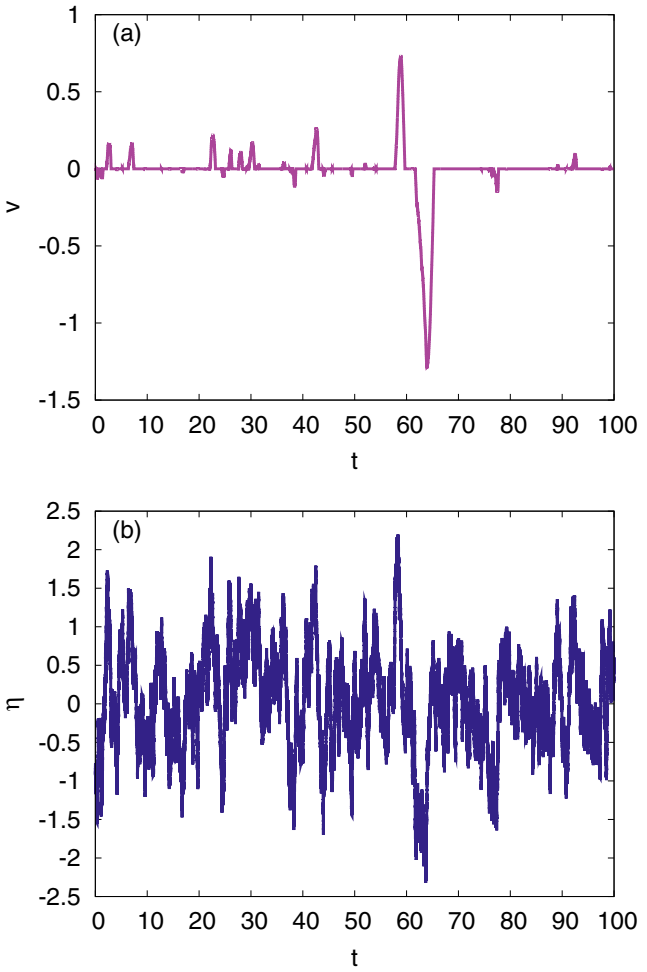

FIG. 3. Time traces of the velocity $v(t)$ (a) and the Ornstein-Uhlenbeck noise $\eta(t)$ (b) of the dry friction model [Eqs. (2) and (3)] for $\tau = 1.0$.

independent kick model [31,32] in studies of dry friction subjected to non-Gaussian noise in the high friction limit [22], and in an experiment of a rotating probe subjected to a granular gas [27]. Intermittent dynamics and a related splitting of the velocity distribution in a regular and a singular part can be clearly seen in numerical studies of the underlying transport equations [33]. Despite the importance of dry friction in engineering, only a few explicit results on its interplay with noisy nonequilibrium environments are available in the literature. We think that justifies a case study like Eq. (3) to uncover potentially general features caused by discontinuities of the flow and noise with a finite amplitude. Furthermore, the noise correlation time τ is used as a continuous control parameter in the analysis of our model. Such a parameter has not been available in the studies using the Boltzmann equation, where only limiting cases of frequent and rare collisions were investigated [26,27,31,32].

III. STATIONARY DENSITY

Given the previous reasoning and the numerical findings, we expect the stationary density to exhibit a singular component caused by particles sticking at $v = 0$. The corresponding stationary distribution is expected to consist of a Dirac δ component at vanishing velocities and $|\eta| < 1$, and a regular part describing moving particles with finite velocities. The analysis will be further hampered by the lack of detailed balance so that closed-form analytic expressions are unlikely to be available.

A. Marginal distribution and unified colored noise approximation

To make some analytical headway, let us first have a look at the marginal velocity distribution $P_v(v) = \int_{-\infty}^{\infty} P(v,\eta)d\eta$ for which perturbative treatments in terms of the correlation time are available. We are interested in possible changes compared to the white-noise case $\tau \neq 0$ (see, e.g., [14]). We apply the unified colored noise approximation (UCNA), developed by Jung and Hänggi [35], to our regularized system Eqs. (2) and (4). This method can be seen as a kind of interpolation scheme for systems with colored noise, as this method shows, under certain conditions, exact results in the limit of vanishing correlation $\tau \to 0$ and high correlation $\tau \to \infty$.

For the convenience of the reader, we recall the main steps of the derivation of the stationary probability density $P_v(v)$. If

we eliminate the variable η from Eqs. (2) and (4), we obtain the second-order equation

$$\ddot{v}(t) + \dot{v}(t)\left(\sigma_\varepsilon'(v(t)) + \frac{1}{\tau}\right) = -\frac{\sigma_\varepsilon(v(t))}{\tau} + \frac{1}{\tau}\xi(t). \tag{5}$$

We introduce a new time scale $\hat{t} = \tau^{-1/2}t$,

$$\ddot{v}(\hat{t}) + \dot{v}(\hat{t})\gamma(v(\hat{t}),\tau) = -\sigma_\varepsilon(v(\hat{t})) + \tau^{-1/4}\xi(\hat{t}), \tag{6}$$

where we have the damping factor

$$\gamma(v,\tau) = \tau^{-1/2} + \tau^{1/2}\sigma_\varepsilon'(v). \tag{7}$$

This factor approaches infinity for both limits $\tau \to 0$ and $\tau \to \infty$. Hence, the setup is suitable for an adiabatic elimination scheme in the limit of small correlation times. If we neglect the second-order derivative, we obtain a simpler multiplicative stochastic process,

$$\dot{v}(\hat{t}) = -\frac{\sigma_\varepsilon(v(\hat{t}))}{\gamma(v(\hat{t}),\tau)} + \frac{1}{\tau^{1/4}\gamma(v(\hat{t}),\tau)}\xi(\hat{t}), \tag{8}$$

with a corresponding Fokker-Planck equation in the Stratonovich sense,

$$\partial_{\hat{t}} P_v = \partial_v\left(\frac{\sigma_\varepsilon(v)}{\gamma(v,\tau)} + \frac{1}{2\tau^{1/2}}\frac{\gamma'(v,\tau)}{\gamma^3(v,\tau)}\right)P_v + \frac{1}{2\tau^{1/2}}\partial_v^2\left(\frac{P_v}{\gamma^2(v,\tau)}\right). \tag{9}$$

Since the adiabatic approximation has reduced the problem to a one-dimensional Fokker-Planck equation, the stationary distribution can be computed by straightforward integration,

$$P_v(v) = \exp\left(-2\int \sigma_\varepsilon(v)dv - \tau\sigma_\varepsilon^2(v) + \ln[|1 + \tau\sigma_\varepsilon'(v)|]\right). \tag{10}$$

In the dry friction limit $\varepsilon \to 0$ the normalized stationary probability density reads

$$P_v(v) = \frac{\exp\left[-2|v| - \tau\sigma_0^2(v)\right][1 + \tau\delta(v)]}{\exp(-\tau) + \sqrt{\pi\tau}\,\mathrm{erf}(\sqrt{\tau})}. \tag{11}$$

Equation (11) shows that the stationary probability density consists of two parts, a regular contribution for $v \neq 0$ and a singular part for $v = 0$. The δ contribution in the density reflects the fact that the particle sticks at $v = 0$ when the stochastic force is not large enough to move the particle. The regular part of the density describes the sliding motion of the particle for $v \neq 0$. By taking the white-noise limit $\tau \to 0$, we arrive at the exact stationary probability density for dry friction with white noise (i.e., [14]). For high correlation times τ, the sliding contribution decreases and the density is mainly determined by the δ peak. Thus, by increasing τ we can observe a gradual transition from sliding to sticking motion. The appearance of a δ peak in the expression for the stationary probability density has also been found in various theoretical studies [20–22,31–33] and in experiments [27].

The accuracy of the perturbative approach can be confirmed by direct numerical simulations; see Fig. 4 for the comparison of the UCNA with direct numerical simulations. By taking about 100 realizations of time traces of length $T = 10^4$, we observe good agreement for small correlation times. However, for values $\tau > 0.1$, deviations between numerics and analytics become visible.

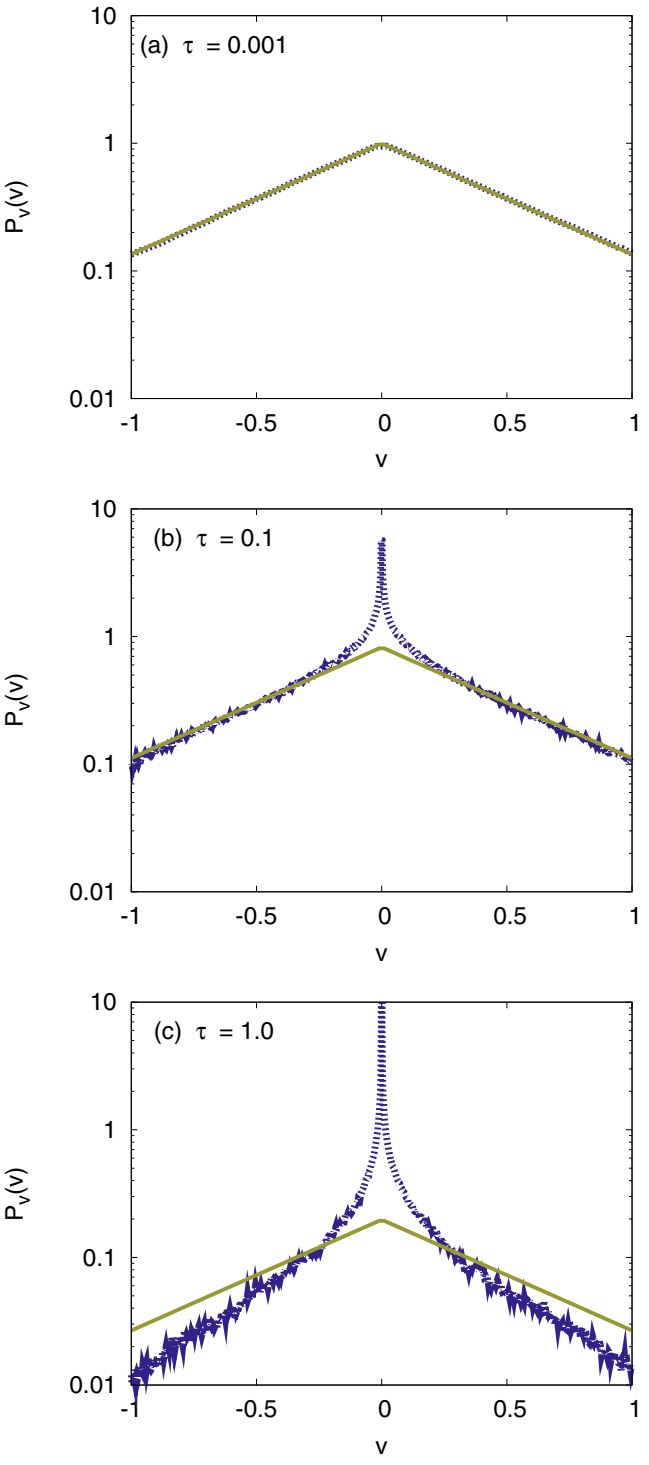

FIG. 4. Regular part of the stationary density, i.e., distribution of the sliding events, obtained from numerical simulations (dashed lines) sampled as a histogram with resolution $\Delta v = 0.002$ and the analytical approximation, Eq. (11) (solid lines). Data have been displayed for different values of the correlation time $\tau = 0.001$ (a), $\tau = 0.1$ (b), and $\tau = 1.0$ (c); cf. Figs. 1–3.

In addition to the analysis of sliding events, Eqs. (10) and (11) also provide an estimate for the singular part, in

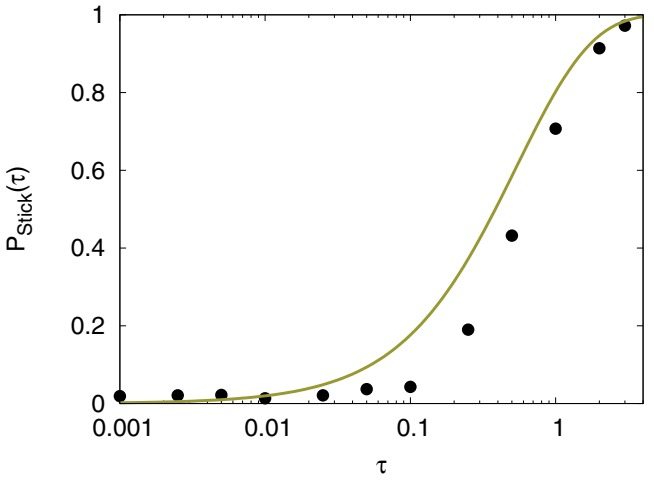

FIG. 5. Probability of the sticking events as a function of the noise correlation time τ. The dots correspond to numerical simulations of Eqs. (2) and (3), and the solid line corresponds to Eq. (12).

particular for the probability of sticking as a function of the noise correlation,

$$P_{\mathrm{Stick}}(\tau) = \frac{\sqrt{\pi\tau}\,\mathrm{erf}(\sqrt{\tau})}{\exp(-\tau) + \sqrt{\pi\tau}\,\mathrm{erf}(\sqrt{\tau})}. \qquad (12)$$

To obtain this result, one needs to integrate the regularized version, Eq. (10), over a small interval containing $v = 0$ and then take the limit $\varepsilon \to 0$. Figure 5 shows a comparison of the analytical approximation with the simulations, and we observe quite good agreement as the probability of sticking increases with increasing τ and approaches the value 1 in the limit of high correlation times.

Overall, the analytic approximation seems to work rather well, especially for small τ. Deviations become visible when the noise correlation time increases (see Fig. 4 for the case $\tau = 1.0$). To explain the deviations between the analytical approximation and the direct numerical simulations for the regular part/sliding events (Fig. 4), we need to take a look at the conditions of validity of the UCNA; this approximation gives proper results for the case $\gamma(v,\tau) \gg 1$. But for higher values of τ, this approximation fails as in our case the contribution caused by the dry friction vanishes in the limit $\varepsilon \to 0$, i.e., when considering the piecewise linear case. Nevertheless, this analytic approximation scheme provides very useful information on the underlying nonequilibrium dynamics of our model.

B. Joint distribution and probability current

To get more insight into the dynamics of our model, we study the two-dimensional equations of motion (2) and (3) with the aim to understand properties of the stationary probability density $P(v,\eta)$.

To begin with, we perform numerical simulations of the dynamics of Eqs. (2) and (3) (see above for details of the numerical integration scheme). Density plots on a logarithmic scale of the full stationary distribution (regular and singular part) are shown in Fig. 6. For $\tau = 0.001$ the singular part hardly matters, and results are almost indistinguishable from the white-noise case within the resolution of our simulations. The regular

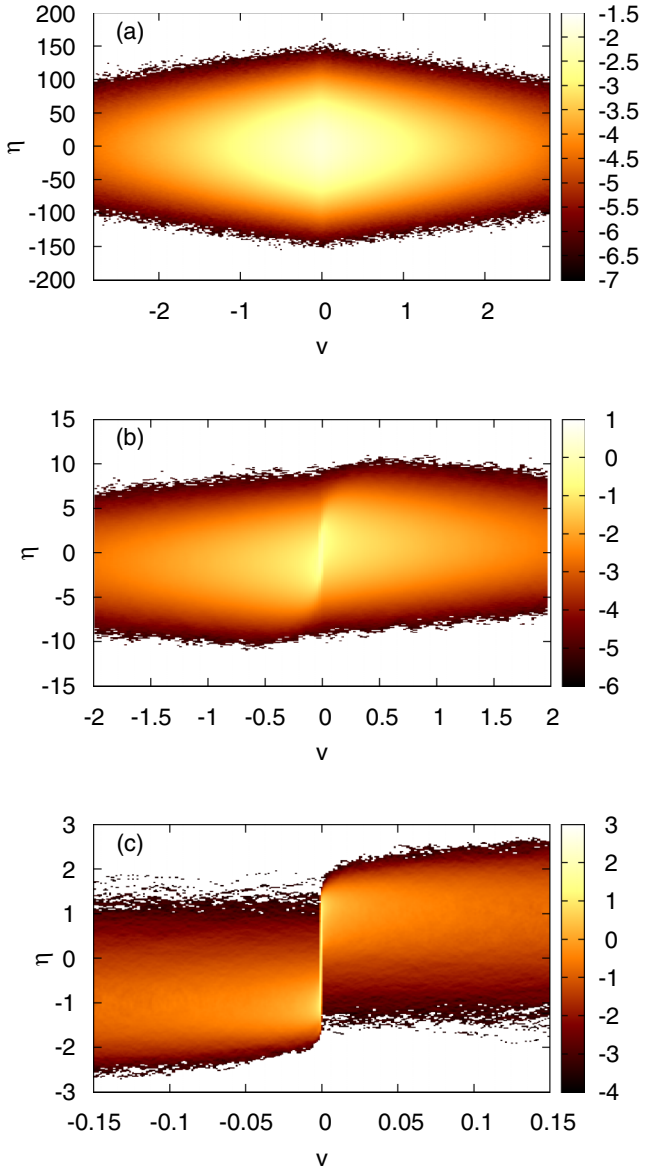

FIG. 6. Logarithmic density plot of the stationary probability density, obtained from numerical simulations of Eqs. (2) and (3), for different values of the correlation time: $\tau = 0.001$ (a), $\tau = 0.1$ (b), and $\tau = 1.0$ (c). The density has been sampled with a resolution of $\Delta v = 0.002$ and 300 bins in the η direction. Slices of the density at $v = 0$ can be found in Fig. 9.

density shows a Gaussian profile in the η direction as well as exponential decay in the v direction. By increasing τ, the density changes significantly as the singular part becomes noticeable [cf. Eq. (11) and Fig. 4]. Furthermore, the regular part of the density becomes asymmetric as the two components in the half-spaces $v > 0$ and $v < 0$ are shifted against each other.

For further analytical insight, we try to formulate the corresponding Fokker-Planck system. Using the regularized version of the equations of motion, Eqs. (2) and (4), the Fokker-Planck equation reads

$$\partial_t P = \partial_v[\sigma_\varepsilon(v) - \eta]P + \partial_\eta\left(\frac{\eta}{\tau} + \frac{1}{2\tau^2}\partial_\eta\right)P. \qquad (13)$$

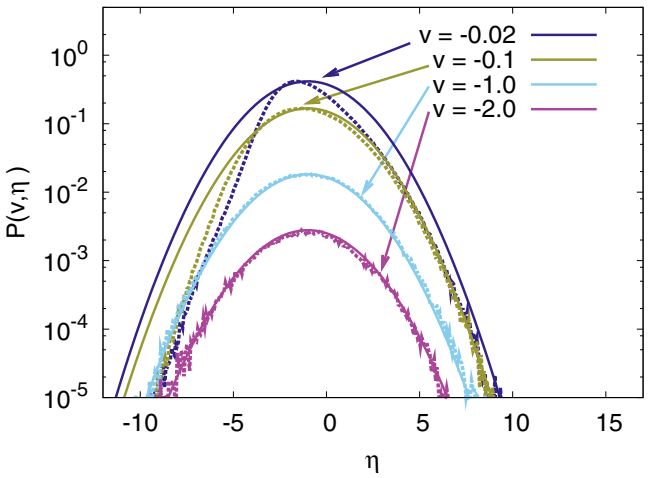

FIG. 7. Regular component of the stationary probability density at $\tau = 0.1$. Dependence on the noise amplitude for different fixed values of the velocity v. Results of numerical simulations (dashed lines) and the analytic asymptotic expression (solid lines), Eq. (15). The normalization of the analytics is fitted to the numerical data.

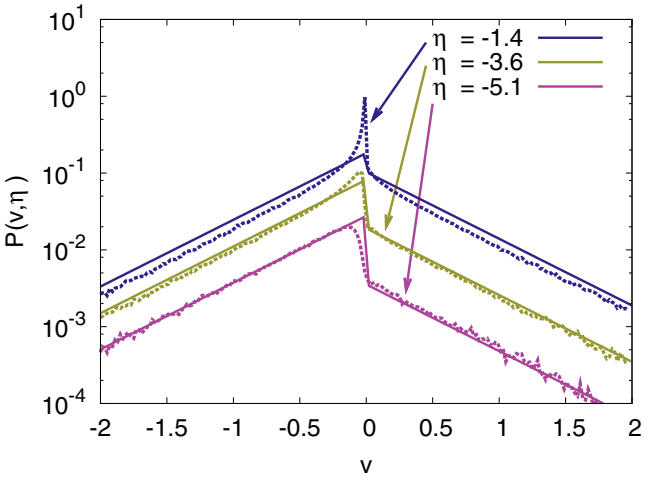

FIG. 8. Regular component of the stationary probability density at $\tau = 0.1$. Dependence on the velocity for different fixed values of the noise amplitude η. Results of numerical simulations (dashed lines) and the analytic asymptotic expression (solid lines), Eq. (15). The normalization of the analytics is fitted to the numerical data.

There is no obvious way to compute the stationary solution because detailed balance is violated. The marginal distribution for the noise amplitude is, however, easily computed as

$$P_\eta(\eta) = \sqrt{\frac{\tau}{\pi}}\exp(-\tau\eta^2) \tag{14}$$

and it does not depend on the regularization. Hence Eq. (14) applies as well in the dry friction limit $\varepsilon \to 0$, which does not come as a surprise [cf. Eq. (2)]. In the dry friction limit, the expression

$$P(v,\eta) = \exp[-2|v| + 2\tau\sigma_0(v)\eta - \tau\eta^2] \tag{15}$$

formally solves the stationary Fokker-Planck equation, see Eq. (13) in the limit $\varepsilon \to 0$, as long as v is nonzero. It differs from the regular part of the marginal [Eq. (11)] by the sign of the mixed (v,η) term. Certainly Eq. (15) does not provide an analytic solution for the stationary density as Eq. (15) does not obey the required matching conditions at $v = 0$ [39]. Nevertheless, if the impact of the stick-slip phenomenon at $v = 0$ remains localized, then Eq. (15) provides the asymptotic behavior for large values of velocities. This assertion can be verified by looking into the numerical data. In Fig. 7, slices of the regular density taken at constant values of the velocity show deviations from the Gaussian profile close to the singular component, i.e., at low velocities. However, the Gaussian profile according to Eq. (15) is restored when we increase the velocity, i.e., at regions in phase space further away from the sticking region. Deviations from the Gaussian profile or strictly speaking the asymmetry of the distribution in the η direction can also be observed in Fig. 6 (bottom) for a high noise correlation τ. A similar feature is displayed by slices taken at a constant noise level; see Fig. 8.

The singular part of the distribution, which means the dynamics of sticking particles, is entirely governed by Eq. (2), i.e., by the Fokker-Planck equation of the Ornstein-Uhlenbeck process. But natural boundary conditions do not apply as particles perform stick-slip transitions. For the singular part of the density at $v = 0$ we have already indicated that increasing the correlation time results in a considerable decrease of the probability of sliding particles. As a result, the main contribution to the marginal distribution, Eq. (14), will come from the density at $v = 0$ as, apart from an exponentially small contribution, particles become immobile. That is in quantitative agreement with direct simulations; see Fig. 9. For small values of the correlation time, considerable deviations from the normal distribution appear as on the one hand particles become mobile frequently and on the other hand there is a constant stream of mobile particles getting stuck (see also Figs. 1–3).

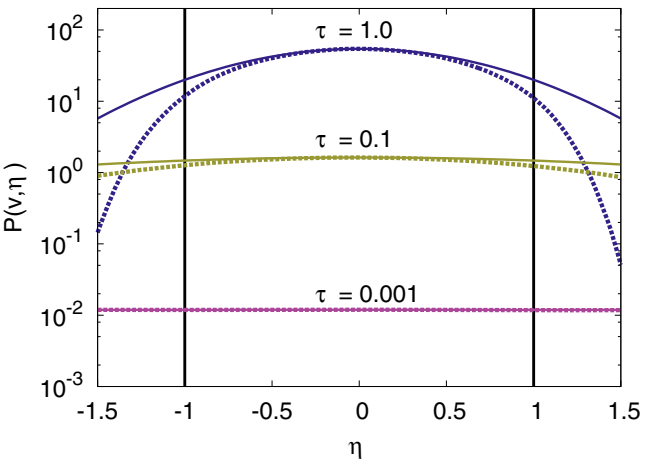

FIG. 9. Slices of the stationary density at $v = 0$ in the η direction, obtained from numerical simulations (dashed lines) and analytic results for the marginal distribution, Eq. (14) (solid lines), for different values of the noise correlation time. The vertical solid lines indicate the region of the singular part of the distribution (sticking regime). The normalization of the analytics is fitted to the numerical data.

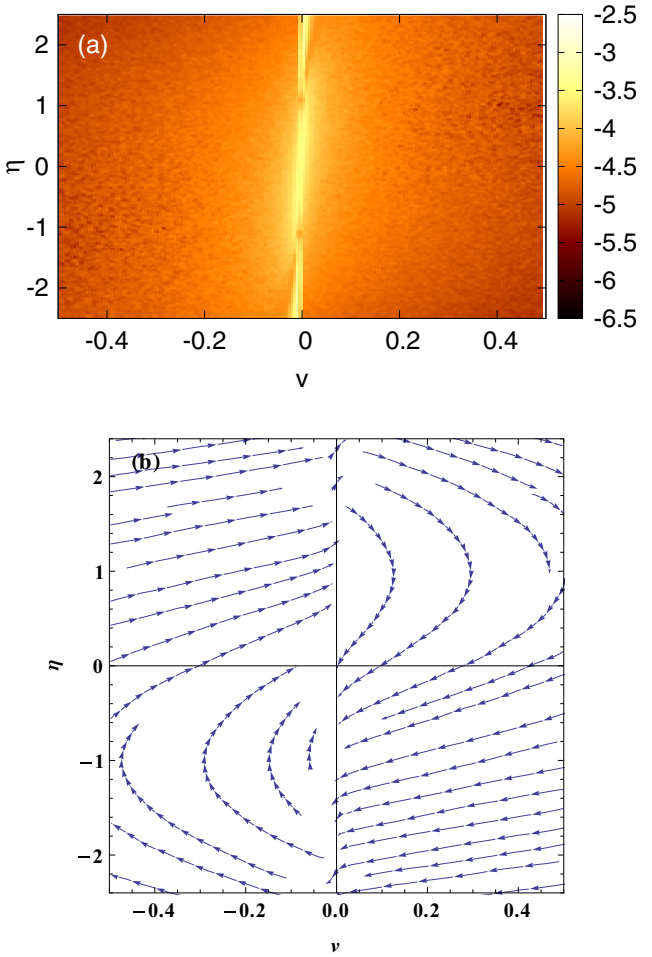

FIG. 10. Logarithmic density plot (a) and stream plot (b) of the regular part of the stationary probability current of the system Eqs. (2) and (3) for $\tau = 0.1$, obtained from numerical simulations. The density plot shows the absolute value of the current in the (v,η) plane, whereas the stream plot displays the normalized vector field of the current.

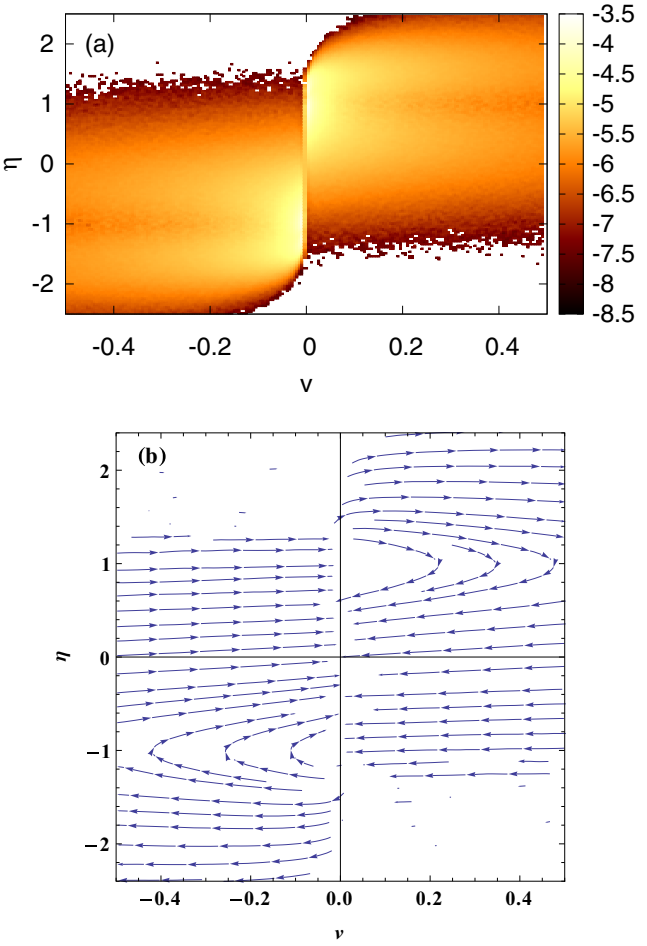

FIG. 11. Logarithmic density plot (a) and stream plot (b) of the regular part of the stationary probability current of the system Eqs. (2) and (3) for $\tau = 1.0$, obtained from numerical simulations. The density plot shows the absolute value of the current in the (v,η) plane, whereas the stream plot displays the normalized vector field of the current.

In the region of the phase space close to the stick-slip transition, the shape of the distribution is affected at intermediate values of the noise correlation. There is no obvious way to tackle the issue by analytical means, e.g., with the matching conditions between the singular and the regular part. But one can at least have a closer look at the probability current, which is a clear signature of the nonequilibrium properties of our model. By using the method from [40], we compute the probability current directly from the time series of our model [Eqs. (2) and (3)] for different values of τ; see Figs. 10 and 11. The entire flow pattern is symmetric, and the main part of the current is concentrated in regions with low velocity v. For $\eta > 1$ the current predominantly points in the positive v-direction as particles are dragged by the external forcing. For larger positive values of v the current turns and finally approaches the sticking manifold $v = 0$, $|\eta| < 1$, where particles change from sliding to sticking mode. As the stationary probability current is, by definition, solenoidal [see Eq. (13)], the current on the sticking manifold becomes large and points in the positive or negative direction; see Fig. 12. When reaching the critical value, $|\eta| = 1$ particles start sliding again. In

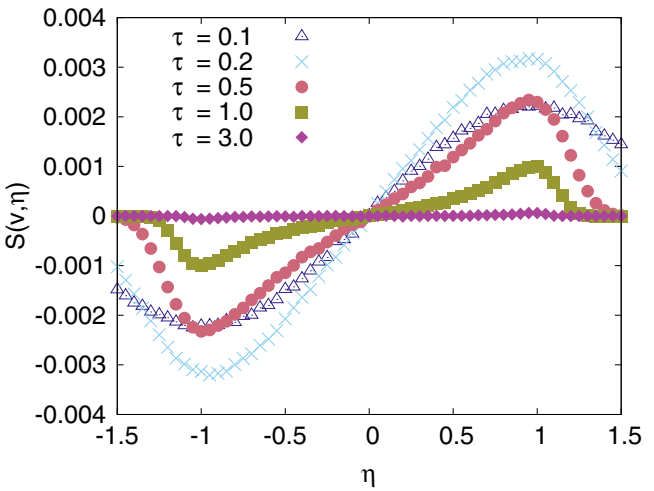

FIG. 12. η component of the stationary probability current at $v = 0$ for different values of τ, obtained from numerical simulations of Eqs. (2) and (3).

particular, the current on the sticking manifold $v = 0$ and $|\eta| < 1$ and the current entering or leaving this manifold obey matching conditions. Hence, for the piecewise-smooth dynamics one can write down a system of two coupled Fokker-Planck equations, one governing the sticking and one governing the sliding motion, with appropriate matching conditions and source terms. It is not obvious, however, whether such a formulation for the regular and the singular component of the probability distribution would give more insight than direct numerical simulations of the associated Langevin equation, let along providing a pathway for an analytic approach.

Figure 12 indicates a nonmonotonic behavior of the current by varying the correlation time of the noise τ. For low values of τ, the current is very small, as we are close to the white-noise limit. By increasing τ the current increases as well up to a value close to $\tau = 0.2$. Increasing τ further, the current decreases and almost vanishes; see the results for $\tau = 3.0$ in Fig. 12. For higher values of the noise correlation, the probability current decays rapidly outside of the interval $\eta \in (-1,1)$. In view of the particular structure of the stationary density this is hardly surprising, as the singular component of the density dominates for high correlation times, the dynamics is dominated by sticking particles, and only a small part of the probability density contributes to the sliding motion and finally to the probability current.

IV. DYNAMICAL PROPERTIES OF THE PIECEWISE LINEAR MODEL

Traditional correlation functions are a useful tool to study dynamical properties, particularly within the context of linear-response theories. From a theoretical perspective, their analytical properties are related with the eigenvalue spectrum of the underlying equations of motion, e.g., with the spectrum of Fokker-Planck operators. Furthermore, correlation functions are experimentally accessible and they allow us to introduce the concept of correlation times. As a shortcoming, correlation functions may not allow for the proper characterization of intermittent behavior, such as stick-slip transitions, which must then be addressed separately by a suitable statistical measure.

A. Power spectral density

To begin with, we want to investigate how the correlation time of the noise τ influences the correlations in our system. To be slightly more precise, we will discuss the τ dependence of the power spectral density of the velocity v, and the corresponding linewidth. The latter provides insight into the structure of the eigenvalue spectrum of an underlying Fokker-Planck operator governing the dynamics of the system. For the dry friction model with white noise ($\tau = 0$), a spectral gap between the two first eigenvalues has been observed [14,41]. In [15] a closed expression for the power spectral density of the velocity has been derived based on the Laplace transform of the propagator.

For noise with a finite correlation time, we mainly rely on numerical investigations since analytic expressions for the stationary probability density are unknown. We calculate the power spectral density of the variable v by averaging over 800 numerically generated time traces of length $T = 10^4$. We base our analysis on the autocorrelations of the velocity. Hence, the corresponding power spectral density predominantly probes properties of the sliding phase as velocities vanish in the sticking phase.

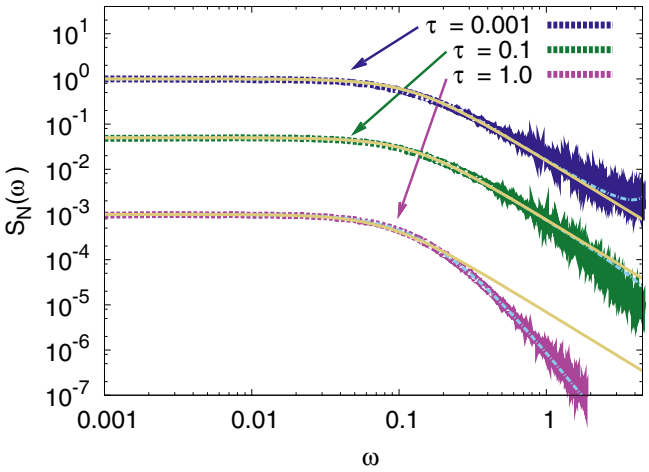

FIG. 13. Double-logarithmic plot of the power spectral density of the v-variable for $\tau = 0.001, 0.1, 1.0$ (from top to bottom) and different fit functions. Spectra have been normalized by the condition $S_N(0) = 1$ and shifted, respectively. Numerical simulations (dashed lines), Lorentzian fit [$\sim 1/(1+\omega^2)$] [(bronze) solid lines], and quartic spectral fit [$\sim 1/(1+a\omega^2+b\omega^4)$] [(cyan) dot-dashed lines].

Figure 13 shows the numerical results of the normalized spectral densities for different values of τ. The normalized power spectral densities $S_N(\omega)$ have a single central peak at $\omega = 0$ indicating an exponential decay of the corresponding autocorrelation function. For small values of τ, and in accordance with the white noise limit, $S_N(\omega)$ is a Lorentzian with power-law behavior ω^{-2} at an intermediate frequency range. Such decay changes when increasing the noise correlation time τ, resulting in a decay proportional to ω^{-4} at medium frequencies. The corresponding analytic behavior indicates a smooth autocorrelation function at time zero.

The complex valued singularities of the power spectral density are signatures of the nonvanishing eigenvalue of an underlying Fokker-Planck operator. For power spectral densities with a well-defined central peak, the full width at half-maximum $\Delta\omega$ can be related to the correlation time of the system t_{corr} via the Wiener-Khinchin theorem. Following results for linear stochastic processes, we define here a correlation time by $t_{\mathrm{corr}} = 1/\Delta\omega$. Using a fit function of the form $1/(1+a\omega^2+b\omega^4)$ for the power spectral densities $S_N(\omega)$, we evaluate the correlation time; see Fig. 14.

The correlation time t_{corr} essentially coincides with the value of the white-noise limit as long as $\tau < 0.1$. While there is no sharp transition, t_{corr} significantly increases monotonically when the noise correlation time exceeds a "critical" value of $\tau = 0.1$. Hence, signatures of the stick-slip transition become dynamically visible above such a critical value. The transition-like feature is in accordance with the findings about the stationary density reported in the previous section, e.g., see Fig. 5.

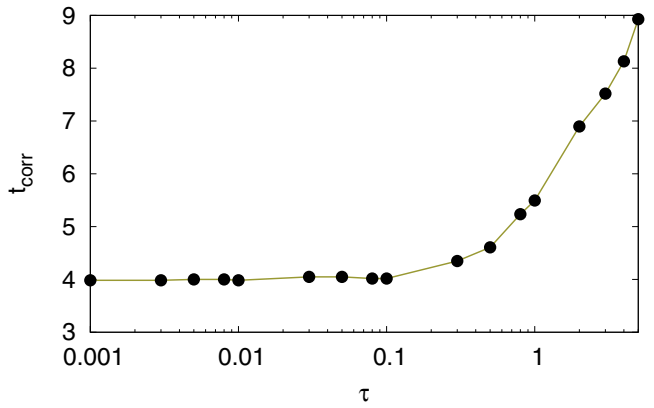

FIG. 14. Correlation time t_{corr} as a function of the noise correlation time τ, obtained from numerical simulations of the spectral density and estimating the full width at half-maximum by using a quartic spectral fit; see Fig. 13.

B. Distribution of sticking and sliding periods

The time traces shown in Figs. 1–3 suggest a closer relation of the dynamics with intermittency phenomena. To probe directly the dynamical features of the stick-slip transition, we look at the distribution of sticking and sliding times, i.e., the distribution of time intervals the particle spends in states $v = 0$ and $v \neq 0$.

We start our investigations with the analysis of the sticking time events. As the dynamics of sticking particles is mainly determined by the exit time problem of the Ornstein-Uhlenbeck process [see Eq. (2)], this problem can be treated by analytical means; see [42]. The Laplace transform of the exit time probability density for an Ornstein-Uhlenbeck process such as Eq. (2) with symmetric absorbing boundaries ($-a$ and a) and a fixed initial condition $|\eta_0| < a$ reads

$$\tilde{f}(s|\eta_0) = \frac{D_{-s\tau}(\sqrt{2\tau}\eta_0)+D_{-s\tau}(-\sqrt{2\tau}\eta_0)}{D_{-s\tau}(\sqrt{2\tau}a)+D_{-s\tau}(-\sqrt{2\tau}a)} \exp\left[\frac{\tau}{2}\left(\eta_0^2 - a\right)\right]$$
$$= \exp\left(\frac{a\tau(a-1)}{2}\right) \frac{{}_1F_1\left(\frac{s\tau}{2};\frac{1}{2};\eta_0^2\tau\right)}{{}_1F_1\left(\frac{s\tau}{2};\frac{1}{2};a^2\tau\right)}, \tag{16}$$

where $D_v(x)$ is the parabolic cylinder function, ${}_1F_1(a;b;z)$ denotes Kummer's confluent hypergeometric function, and we have used some identities for these functions [43]. We set $a = 1$ because the regime where particles are sticking is the interval $(-1,1)$, and we integrate over all possible initial conditions η_0 within this regime assuming a uniform distribution to obtain

$$\tilde{f}(s) = \frac{1}{2}\int_{-1}^{1} \tilde{f}(s|\eta_0)d\eta_0$$
$$= \frac{{}_1F_1\left(\frac{s\tau}{2};\frac{3}{2};\tau\right)}{{}_1F_1\left(\frac{s\tau}{2};\frac{1}{2};\tau\right)}. \tag{17}$$

As it is not possible to derive an analytic result for the inverse Laplace transform of this expression, we use the Talbot method to calculate the exit time distribution numerically [44,45]. The results for certain values of τ are shown in Figs. 15–17. One observes a localized peak in the distribution at $T = 0$, and for moderate to large times a simple exponential decay.

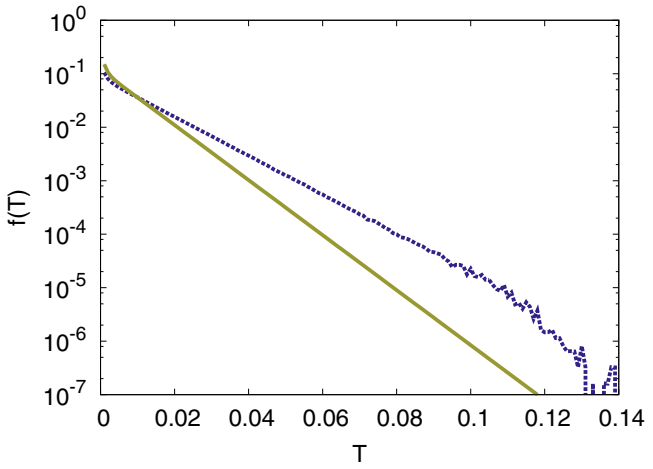

FIG. 15. Distribution of sticking time intervals, $f(T)$, on a semilogarithmic scale for $\tau = 0.1$, obtained numerically [(blue) dashed line] and semianalytically from the exit time problem for the Ornstein-Uhlenbeck process [(bronze) solid line] [the inverse Laplace transform of Eq. (17)].

For higher noise correlation times, the exponential decay of the distribution becomes smaller. It becomes more likely for particles to stick at $v = 0$, which is in accordance with the results in the previous sections. Our numerical findings for the exit time distribution agree very well with the analytical estimate, i.e., the inverse Laplace transform of Eq. (17). It works particularly well for large values of τ and fails to be valid if we approach the transition value $\tau = 0.1$ as stick-slip phenomena become noticeable around this value.

For the remainder of this section, we focus on the statistics of the sliding events. Figures 18 and 19 show the numerically obtained distributions over a wide range of noise correlation times. For small noise correlation, distributions are unimodal with a power-law decay at an intermediate range. For a larger

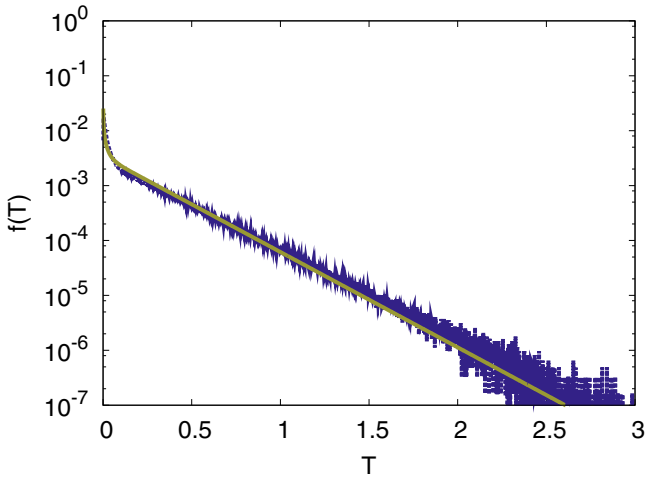

FIG. 16. Distribution of sticking time intervals, $f(T)$, on a semilogarithmic scale for $\tau = 0.5$, obtained numerically [(blue) dashed line] and semianalytically from the exit time problem for the Ornstein-Uhlenbeck process [(bronze) solid line] [the inverse Laplace transform of Eq. (17)].

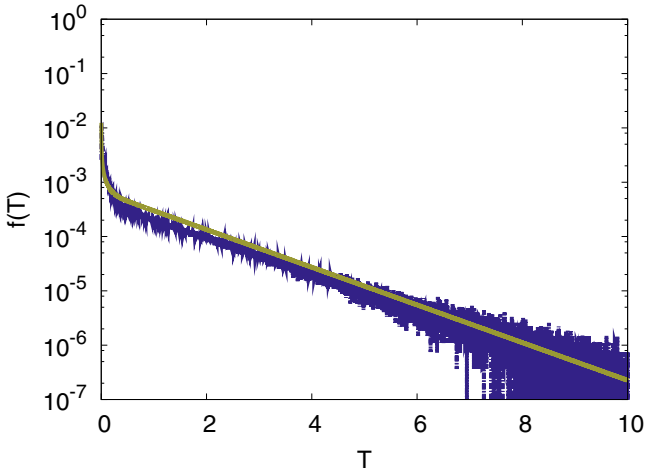

FIG. 17. Distribution of sticking time intervals, $f(T)$, on a semilogarithmic scale for $\tau = 1.0$, obtained numerically [(blue) dashed line] and semianalytically from the exit time problem for the Ornstein-Uhlenbeck process [(bronze) solid line] [the inverse Laplace transform of Eq. (17)].

noise correlation, the distributions develop a maximum at a finite time so that the most probable sliding time becomes finite. Figure 19 indicates a kind of universal behavior of the distributions at long sliding times T for large correlation times τ. The asymptotic behavior of the distributions shows a stunning similarity to characteristics of on-off intermittency [46] as the power-law decay is of the form $T^{-3/2}$ for $\tau \geqslant 1.0$. But in the context of our model, the roles of the "on" and "off" states are interchanged as this power law occurs for sliding events. Looking for an analytic approach, the sliding events could be modeled by an exit time problem with constant drift and colored noise. For Gaussian white noise and constant drift, this problem can be solved analytically [47], and the exit time distribution shows an asymptotic behavior $P(T, v_0) \sim T^{-3/2} \exp[-(T - v_0)^2/2T]$.

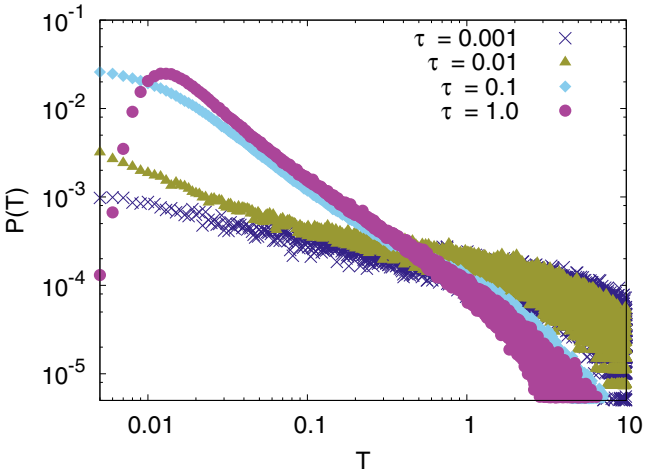

FIG. 18. Distribution of sliding time intervals, $P(T)$, on a double-logarithmic scale for different values of the noise correlation time, obtained from numerical simulations.

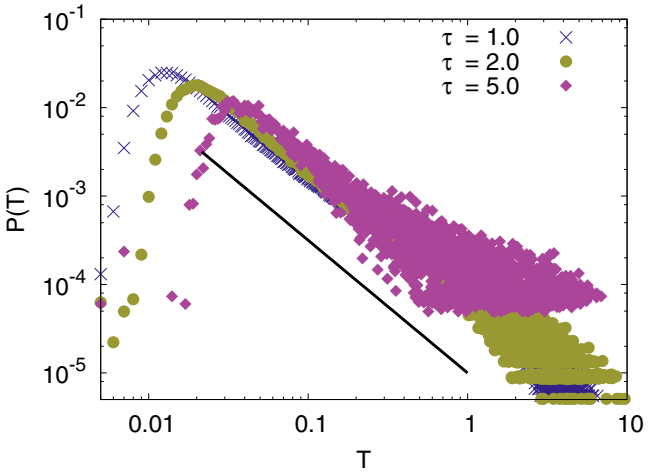

FIG. 19. Distribution of sliding time intervals, $P(T)$, on a double-logarithmic scale for different values of the noise correlation time, obtained from numerical simulations. The black line shows a decay according to a power law $T^{-3/2}$.

V. CONCLUSION

We investigated a dry friction model subjected to colored noise with the emphasis on nonequilibrium properties in a noisy piecewise-smooth dynamical system. By applying the unified colored noise approximation (UCNA), we obtained an analytical expression of the stationary probability density for the velocity. The white-noise limit $\tau \to 0$ reproduces the exact results, e.g., see [11]. As the noise correlation time increases, the stationary density develops a δ peak as particles become more and more stuck at $v = 0$. By varying τ, a transition from sliding to sticking dynamics could be observed. By considering the equivalent two-dimensional system, we were able to derive an asymptotic expression for the stationary density that is valid for large velocities and large noise amplitudes, far away from the stick-slip region. There was no obvious way to obtain a full analytic expression for the joint probability density $P(v, \eta)$ containing all the required matching conditions at $v = 0$ as detailed balance is violated. The latter has been clearly demonstrated by computing the nonvanishing stationary probability current.

Furthermore, we studied the power spectral density numerically to obtain information about the velocity correlations, the corresponding correlation time, and the spectral gap of the underlying Fokker-Planck operator. Below a "critical value" one recovers the result for the white-noise limit. Increasing the noise correlation further, the full width at half-maximum decreases, which is connected to a higher velocity correlation in the system. This decrease of the spectral width comes along with a change in shape of the power spectrum. For low values of τ the power spectral density is a Lorentzian, while for values $\tau > 0.1$ the shape changes to a ω^{-4} decay for intermediate frequencies.

To complete our studies, we investigated the sliding and sticking time distribution as the time traces indicated a connection to intermittent dynamics. Results for the sticking time distribution were accessible via the exit time problem for an Ornstein-Uhlenbeck process with symmetric absorbing boundary conditions. For the sliding dynamics, the related exit

time problem with colored noise and a constant drift is hard to tackle, and we had to rely on simulations. For high noise correlation times, a power-law decay of the form $T^{-3/2}$ occurs, indicating a relation with on-off intermittency.

References [26] and [27] provide probably the most comprehensive experimental and theoretical analysis of a device subjected to dry friction and a nonequilibrium granular heat bath. The corresponding theoretical considerations have been based on a Boltzmann equation approach. Results such as a ratchet effect induced by geometric asymmetries and the localization of the velocity distribution are in accordance with measurements. Given the sophisticated nature of the underlying theoretical description, time correlations and power spectra are not accessible by analytic methods.

In our analysis, we have addressed a simpler but related theoretical model using colored noise instead of a collision integral. There is no mathematical link between both models, and the Boltzmann equation and the dry friction model subjected to colored noise are fundamentally different. Nevertheless, we found various striking similarities. Time traces of the colored noise model are surprisingly similar to those measured in experiments if the cases of rare and frequent collision limits are compared with large and small noise correlation time. In addition, both models produce densities with a singular component caused by the discontinuous drift, a feature that is common in a large class of piecewise-smooth stochastic models; see, e.g., [21]. Such a property can be seen as a ubiquitous feature of stick-slip phenomena, which is not restricted to a particular theoretical or experimental realization.

Within the analysis of the dry friction model subjected to colored noise, we were able to derive an analytic expression for the weight of the singular component, which is otherwise hardly accessible (see, e.g., [21]). The analysis of the colored noise model is facilitated by a continuous control parameter, which has not been available in the aforementioned more realistic studies, where only the limiting cases of frequent and rare collisions could be addressed. We were able to identify a critical noise correlation time separating the white-noise regime from models where noise correlations have a visible effect in the presence of discontinuous drifts. Our model allowed for a detailed analysis of nonequilibrium currents and power spectra. In particular, the on-off intermittent characteristics is a promising result that is tempting to check experimentally. In addition to the setup used in [27], a realization along the lines of [25] would allow us to implement noise color quantitatively and thus would provide a direct experimental comparison.

Apart from experimental confirmations, the colored noise model is remarkable as well from a plain theoretical perspective. In the extended (v,η) phase space, the model is described by a plain Fokker-Planck equation. Because of the particular structure of diffusion and discontinuous drift, the two-dimensional Gaussian white-noise model develops a singular stationary density, proving that such a localization phenomenon is by no means a feature that requires more complicated noise sources. Hence, features previously found in Boltzmann equations can be certainly captured by Fokker-Planck equations and simpler stochastic models, which may be amenable for an analytic treatment.

[1] M. di Bernardo, C. J. Budd, A. R. Champneys, and P. Kowalczyk, *Piecewise-smooth Dynamical Systems: Theory and Applications* (Springer, Berlin, 2008).

[2] A. F. Filippov, *Differential Equations with Discontinuous Righthand Sides* (Kluwer, Dordrecht, 1988).

[3] O. Makarenkov and J. S. W. Lamb, Physica D **241**, 1826 (2012).

[4] S. Coombes, R. Thul, and K. C. A. Wedgwood, Physica D **241**, 2042 (2012).

[5] M. R. Jeffrey, Phys. Rev. Lett. **106**, 254103 (2011).

[6] J. J. B. Biemond, N. van de Wouw, and H. Nijmeijer, Physica D **241**, 1882 (2012).

[7] F. P. Bowden and D. Tabor, *The Friction and Lubrication of Solids* (Oxford University Press, Oxford, 1950).

[8] F.-J. Elmer, J. Phys. A **30**, 6057 (1997).

[9] C. Wensrich, Tribol. Intern. **39**, 490 (2006).

[10] A. Kawarada and H. Hayakawa, J. Phys. Soc. Jpn. **73**, 2037 (2004).

[11] P.-G. de Gennes, J. Stat. Phys. **119**, 953 (2005).

[12] H. Hayakawa, Physica D **205**, 48 (2005).

[13] T. K. Caughey and J. K. Dienes, J. Appl. Phys. **32**, 2476 (1961).

[14] H. Touchette, E. van der Straeten, and W. Just, J. Phys. A **43**, 445002 (2010).

[15] H. Touchette, T. Prellberg, and W. Just, J. Phys. A **45**, 395002 (2012).

[16] A. Baule, E. G. D. Cohen, and H. Touchette, J. Phys. A **43**, 025003 (2010).

[17] A. Baule, H. Touchette, and E. G. D. Cohen, Nonlinearity **24**, 351 (2011).

[18] Y. Chen, A. Baule, H. Touchette, and W. Just, Phys. Rev. E **88**, 052103 (2013).

[19] Y. Chen and W. Just, Phys. Rev. E **89**, 022103 (2014).

[20] A. Baule and P. Sollich, Europhys. Lett. **97**, 20001 (2012).

[21] A. Baule and P. Sollich, Phys. Rev. E **87**, 032112 (2013).

[22] K. Kanazawa, T. G. Sano, T. Sagawa, and H. Hayakawa, J. Stat. Phys. **160**, 1294 (2015).

[23] M. K. Chaudhury and S. Mettu, Langmuir **24**, 6128 (2008).

[24] P. S. Goohpattader, S. Mettu, and M. K. Chaudhury, Langmuir **25**, 9969 (2009).

[25] P. S. Goohpattader and M. K. Chaudhury, J. Chem. Phys. **133**, 024702 (2010).

[26] A. Gnoli, A. Petri, F. Dalton, G. Pontuale, G. Gradenigo, A. Sarracino, and A. Puglisi, Phys. Rev. Lett. **110**, 120601 (2013).

[27] A. Gnoli, A. Puglisi, and H. Touchette, Europhys. Lett. **102**, 14002 (2013).

[28] D. J. W. Simpson and R. Kuske, Discrete Contin. Dyn. Syst. Ser. B **19**, 2889 (2014).

[29] D. J. W. Simpson and R. Kuske, J. Nonlin. Sci. **25**, 967 (2015).

[30] P. Eshuis, K. van der Weele, D. Lohse, and D. van der Meer, Phys. Rev. Lett. **104**, 248001 (2010).

[31] J. Talbot, R. D. Wildman, and P. Viot, Phys. Rev. Lett. **107**, 138001 (2011).

[32] J. Talbot and P. Viot, Phys. Rev. E **85**, 021310 (2012).

[33] T. G. Sano, K. Kanazawa, and H. Hayakawa, Phys. Rev. E **94**, 032910 (2016).
[34] P. Hänggi and P. Jung, Adv. Chem. Phys. **89**, 239 (1995).
[35] P. Jung and P. Hänggi, Phys. Rev. A **35**, 4464(R) (1987).
[36] R. Kubo, in *Fluctuation, Relaxation and Resonance in Magnetic Systems*, edited by D. ter Haar (Oliver and Boyd, Edinburgh, 1962), pp. 23–68.
[37] S. Brandstetter, M. A. Dahlem, and E. Schöll, Philos. Trans. R. Soc. A **368**, 391 (2010).
[38] R. Kubo, M. Toda, and N. Hashitsume, *Statistical Physics II: Nonequilibrium Statistical Mechanics* (Springer, Berlin, 1991).
[39] C. Gardiner, *Stochastic Methods: A Handbook for the Natural and Social Sciences* (Springer, Berlin, 2009).
[40] W. Just, H. Kantz, M. Ragwitz, and F. Schmüser, Europhys. Lett. **62**, 28 (2003).
[41] H. Risken, *The Fokker-Planck Equation: Methods of Solution and Applications* (Springer, Berlin, 1989).
[42] D. A. Darling and A. J. F. Siegert, Ann. Math. Stat. **24**, 624 (1953).
[43] M. Abramowitz and I. A. Stegun, *Handbook of Mathematical Functions* (Dover, New York, 1970).
[44] A. Talbot, IMA J. Appl. Math. **23**, 97 (1979).
[45] J. Abate and P. P. Valkó, Int. J. Numer. Methods **60**, 979 (2004).
[46] J. F. Heagy, N. Platt, and S. M. Hammel, Phys. Rev. E **49**, 1140 (1994).
[47] S. N. Majumdar and A. Comtet, Phys. Rev. E **66**, 061105 (2002).